Colloids and Surfaces A 601 (2020) 124989

Contents lists available at ScienceDirect

Colloids and Surfaces A

journal homepage: www.elsevier.com/locate/colsurfa

Analysis of dilution induced disintegration of micellar drug carriers in the presence of inter and intra micellar species

Hurriyet Polat[a,*], Gulistan Kutluay[a], Mehmet Polat[b]

[a] Department of Chemistry, Izmir Institute of Technology, Urla, Izmir, Turkey
[b] Department of Chemical Engineering, Izmir Institute of Technology, Urla, Izmir, Turkey

GRAPHICAL ABSTRACT

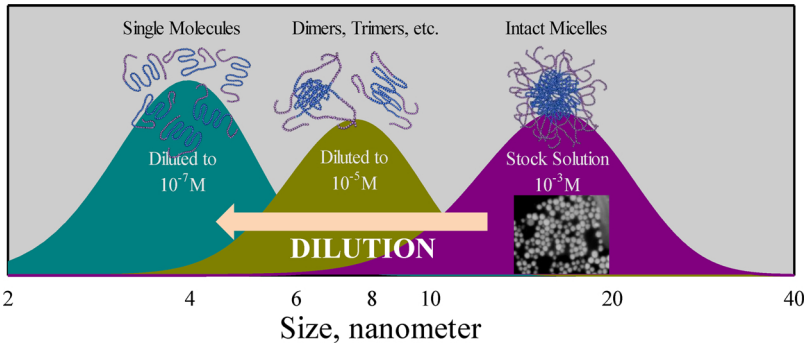

ARTICLE INFO

Keywords:
Micelles
Polymeric surfactant
Drug carrier
Stability
Protein

ABSTRACT

Micelles of self-assembling polymeric surfactant molecules are promising nanoscopic carriers for lipophilic and toxic drugs, genes, and imaging molecules. Though it is a must for successful transport, ensuring micelle integrity is a challenge during intravenous injection where micelles must endure abrupt dilutional effects and encounters with native molecules. Therefore, direct observational evidence of how micelles behave during dilution is valuable in manipulating the designs of these carriers for a succesful drug delivery.

Morphology and stability of the barren and a drug-loaded (lipophilic probucol) micelles of a polymeric surfactant (Pluronic® P123) were monitored during systematic re-dilution in distilled water and simulated body fluid in the presence of a model protein (bovine serum albumin). It was observed through surface tension, dynamic light scattering, laser velocimetry, transmission scanning and transmission electron microscopy, and atomic force microscopy analyses that the micelles disintegrated to various degrees in all cases upon dilution. The results indicate that dilution effects must be taken into account in designing micellar drug carriers. The assistance of some other means of protection such as encapsulation should be considered for ensuring micelle integrity within the bloodstream.

1. Introduction

Therapeutic compounds with low water solubility require delivery agents for efficient inclusion and transport in aqueous body fluids. Amphiphilic block copolymers which contain chemically tethered hydrophilic and hydrophobic segments have been used extensively for this

* Corresponding author.
E-mail addresses: hurriyetpolat@iyte.edu.tr (H. Polat), mehmetpolat@iyte.edu.tr (M. Polat).

https://doi.org/10.1016/j.colsurfa.2020.124989
Received 26 March 2020; Received in revised form 6 May 2020; Accepted 8 May 2020
Available online 19 May 2020
0927-7757/

Table 1
A summary of the chemicals employed in the study.

Name/Formula	Chemical Structure	MW g/mole
Tri-block copolymer (P123) $HO(EO)_{20}(PO)_{70}(EO)_{20}H$	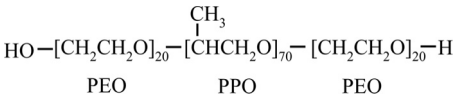	5800
Probucol $C_{31}H_{48}O_2S_2$	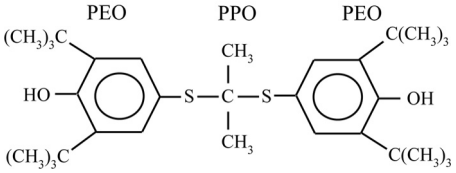	516.8
Acetonitrile CH_3CN	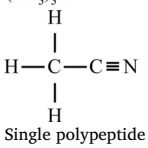	41.1
Bovine serum albumin (BSA)	Single polypeptide chain consisting of 583 amino acid residues	66,463

purpose. In aqueous solutions, these polymers associate into nano-sized core/shell structures called micelles above a critical concentration (the Critical Micelle Concentration or CMC). The hydrophobic core section of a micelle serves as a container for the lipophilic drug molecules whereas the hydrophilic shell (corona) provides water solubility. Among the wide spectrum of block copolymers, Pluronic® series of surfactants are preferred since they exhibit excellent biodegradability, relatively small critical micelle concentrations, and better drug loading properties.

Theoretically, once stabilized inside the micellar cores, the probability of the drug molecules avoiding premature degradation and ingestion before reaching the target tissues is expected to increase. However, it has been routinely observed that the efficiency of the micelles as drug-carriers is lower than desired [1–8]. The low efficiency has been attributed to various factors such as the micelle structure, drug type, and degree of interaction between the drug molecules and the micelles. Another obvious reason is the interaction of the micelles with the native blood plasma components.

If present, such interactions may alter the conformation, size, and surface properties of the carrier and negatively influence both the drug holding capacity and activity at the target site. The most potent binding partners in the blood are albumin, immunoglobulins, fibrinogen, apolipoproteins, and complement cascade proteins [1,9–11]. Serum albumin is a particularly important example with its ability to bind easily to other compounds and a very high plasma concentration between 30–50 grams per liter [12]. Kabanov et al. [13] state that direct characterization of the micelle stability *in vivo* is next to impossible due to difficulties in discriminating micelles from the native species of the blood plasma such as cells, proteins, and other macromolecules. Therefore, the bulk of the data on polymeric surfactant molecules and the stability of their micelles are limited to *in vitro* studies, a majority of which is carried out in distilled water and focusing on either protein-protein [14–21] or protein-simple surfactant interactions [21–31]. Comprehensive reviews by Owen et al. [30], Shi et al. [31], and Zhou et al. [32] addressing these issues and suggesting strategies for sustained drug delivery are present in the literature.

Another potential reason for the low efficiency of the micellar carriers is the unavoidable dilution the micelles encounter when introduced into the blood stream. Kobanov et al. [13] suggest that dilution-related disintegration of the drug-bearing micelles may be responsible for diminishing the amount of drug which can be successfully transferred by the carrier. Nevertheless, the risk of disintegration has been played down in the literature, presuming that the rate of micellar dissociation will be slow enough to allow sufficient transfer.

This study aims at a systematic characterization of the stability of barren or a lipophilic drug-loaded (probucol) tri-block copolymer micelles (Pluronic P123) under dilution conditions of varying severity in distilled water and simulated body fluids. The effect of the presence of a model binding agent (bovine serum albumin-BSA) was also comparatively examined. The micelle morphology and stability was determined directly by examining the size, morphology and physicochemical structure of the micelles through surface tension, dynamic light scattering, laser velocimetry, transmission scanning and transmission electron microscopy, and atomic force microscopy measurements. The data presented here provide a quantitative description of the effect of dilution on the stability of micellar structures for drug delivery applications.

2. Materials and methods

2.1. Materials

A Pluronic series tri-block copolymeric surfactant (P123) was employed to form the micelles. Besides the relatively high micellar stability within the Pluronic group of surfactants, P123 is an attractive choice as a drug carrier due to its longer hydrophobic blocks, which provide a more receptive environment for the drug molecules, its commercial availability and biocompatibility [33,34]. The micelles were initially formed in distilled water or simulated body fluids to have micellar stock solutions at a surfactant concentration of 10^{-3} M P123 (see Section 2.3 below).

A strongly hydrophobic phenol (probucol) was the model drug. Probucol is an anti-hyperlipidemic drug that functions by lowering the cholesterol level in the blood by inhibiting cholesterol synthesis and delaying cholesterol absorption. It is freely soluble in chloroform, benzene, ether, acetone, ethanol, methanol and acetonitrile, but completely insoluble in water. Concentration of probucol was kept constant at 2.0×10^{-4} M (in the micellar stock solution) when present.

Albumin from bovine serum (BSA) was used as the model protein. This large globular protein which consists of a single polypeptide chain is negatively charged in water and readily soluble. Its concentration was varied in the tests by ten-fold between 10^{-2} M and 10^{-5} M (in the micellar stock solution). Acetonitrile was employed as an environment for co-solving the drug with the block copolymer prior to micelle formation. All the chemicals were supplied by Sigma Aldrich chemical company and their basic properties are presented in Table 1.

Ultra-pure water of 18.2 MΩ. cm^{-1} (DW) at the physiological pH of 7.4 was used throughout the study. The simulated body fluid (SBF) is an electrolyte solution with an ionic strength similar to that of the human blood plasma. It was buffered at pH 7.4 with 50 mM tris-hydroxy methylaminomethane (Tris or THAM, $(HOCH_2)_3CNH_2$) and 45 mM hydrochloric acid at 37 °C [35]. The composition of the body fluid

Table 2
Composition of the body fluid prepared.

Reagent (added in the order listed)	Amount in 1 Liter
NaCl	7.996 gm
$NaHCO_3$	0.350 gm
KCl	0.224 gm
$K_2HPO_4.3H_20$	0.228 gm
$MgCl_2.6H_2O$	0.305 gm
HCl (1 M)	40 ml
$CaCl_2$	0.278 gm
Na_2SO_4	0.071 gm
Tris	6.057 gm

prepared for this study is presented in Table 2.

The carbon grids for the STEM and TEM characterization work were provided by Micro to Nano Innovative Microscopy Supplies from the Netherlands. The mica surfaces used in the AFM scans were provided by WiTec in Germany. They were atomically smooth with an Ra value of 1.26 nm as determined with the AFM analysis.

2.2. Characterization studies

The morphology, size and surface charge of the micelles were characterized both in distilled water and in simulated body fluids using various characterization methods (Table 3). The tests were repeated with barren and drug-loaded micelles in the absence and presence of BSA. The solution preparations and the subsequent measurements were carried out at a solution temperature of 20 °C.

2.3. Preparation and characterization of barren micelles

The micellar solutions were prepared in distilled water and simulated body fluids by adjusting the surfactant concentration to 10^{-3} M. This concentration, which is about a ten times the CMC for this surfactant, is high enough to ensure well-developed spherical micelles and low enough to prevent cylindrical structures. The CMC was verified by surface tension measurements.

The DLS measurement provided in-situ size distributions of the micelles. The micelles were immobilized on carbon grids for STEM and TEM, and on atomically smooth hydrophobic mica surfaces for AFM scans by immersing these surfaces in the micelle solutions for 15 s. The micelle-bearing surfaces were dried and kept under vacuum before the measurements. The STEM, TEM and AFM analyses provided direct information on the size and shape of the micelles.

2.4. Preparation and characterization of pregnant micelles

The loading of the lipophilic drug (probucol) into the P123 micelles was achieved by thin-film hydration procedure. Due to its amphoteric nature which allows it to react both as a base and as an acid, P123 was co-dissolved with the lipophilic drug in copious amounts of acetonitrile. Subsequent evaporation of the solvent generated an organic film of the polymer-drug composite. The composite was then hydrated in either DW or SBF to form the micelles. During hydration, the lipophilic drug molecules are energetically forced into the hydrophobic cores of the micelles, which in turn dissolve in the aqueous phase. The final solution concentrations of the surfactant and the drug were 10^{-3} M and 2×10^{-4} M, respectively. These solutions were used as stock solutions for the subsequent dilution tests.

3. Results and discussion

3.1. Characterization of P123 micelles in DW and SBF solutions

3.1.1. Surface tension measurements

The data in the literature suggest that the monomers of the Pluronic series of surfactants are compact, possibly with the PEO chains forming a relatively tight shell around the non-hydrated PPO core. Brown et al. [36] determined the hydrodynamic radii of the Pluronic P85 (PEO_{26}-PPO_{40}-PEO_{26}) monomers as 1.8 nm at ambient temperature. Their value was similar to that (2.3 nm) observed by Zhou and Chu [37] for Pluronic P188 (PEO_{80}-PPO_{25}-PEO_{80}). These measurements agree relatively well with the theoretically determined gyration (1.7 nm) and hard-sphere (1.15 nm) radii for these class of surfactants [38,39].

The monomers of the Pluronic series of surfactants start aggregating at concentrations as low as 10^{-5} M by creating dimers, trimers, etc. until they reach a concentration around 10^{-3} M where they form compact, fully developed spherical micelles. This behavior is schematically pictured as a representative surface tension profile in the inset curve in Fig. 1 which consists of three distinct regions [40]. In Region 1, the surfactant molecules are in monomeric form and strongly adsorb at the air-water interface, surface tension decreasing linearly with concentration. In Region 2, the molecules start to aggregate and their packing density at the interface is changed, causing a variation in the slope of the surface tension curve. Once a critical concentration (CMC) is reached, the surfactant form fully developed aggregates (micelles). Any further concentration increase only causes the formation of new micelles while the relative activitiy of the monomers in the solution and at the interface remains constant. Hence, the surface tension becomes independent of surfactant concentration in Region 3. The formation of polymolecular aggregates in the PEO-PPO-PEO block copolymers solutions have been independently demonstrated through surface tension 40., light scattering and fluorescence spectroscopy experiments [38,41]. Brown et al. [36] reported that dynamic light scattering measurements showed the coexistence of the monomers, micellar aggregates, and micelles in relative proportions which depend critically on temperature and concentration. Similarly, Zhou and Chu [37] with Pluronic P68 and Polat et al. [40] with Pluronic L64, P104, and L44 observed unimer, transitions and micelle regions in their solutions.

In this study, the P123 surface tension profiles were re-created using a surface tensiometer to accurately determine the CMC concentrations in the DW and SBF solutions. The results are presented in Fig. 1. The small figure in the box display the general trend discussed in the previous paragraph for illustration purposes. It can be observed that the P123 molecules are in the monomeric form at a surfactant concentration below 10^{-6} M. The polymeric aggregates begin to develop after this concentration and the micelle formation seems to be achieved at a surfactant concentration of 1.2×10^{-4} M.

Though the CMC and the final surface tension values above the CMC are nearly the same for both the DW and SBF solutions (1.5×10^{-4} M

Table 3
Methods employed in the study in micelle characterization.

Analysis	Method	Device
Surface Tension	Dü Noüy Ring	Krüss Tensiometer K10ST
Size	Dynamic Light Scattering DLS	Malvern Zetasizer Nano ZS
Charge	Laser Doppler Velocimetry DLS-LDV	Malvern Zetasizer Nano ZS
Morphology	Scanning Transmission Electron Microscopy STEM	Quanta 250 SEM
	Transmission Electron Microscopy TEM	FEI Tecnai G2 Spirit Bio Twin
	Atomic Force Microscopy AFM	Bruker Nanoscope8

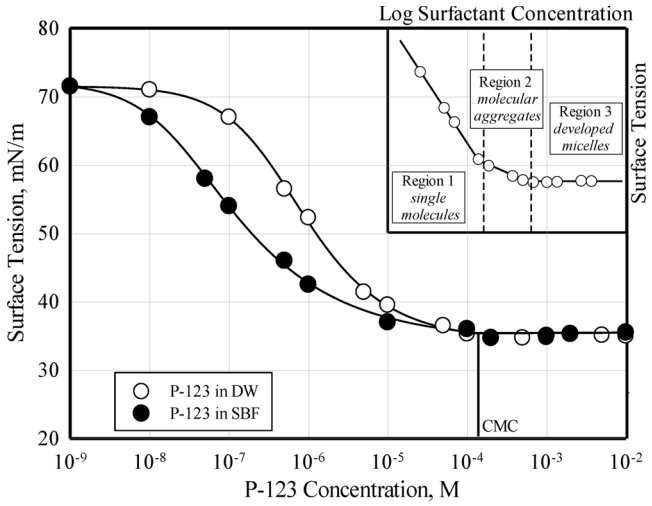

Fig. 1. Surface tension results of P123 in distilled water and SBF.

and 36 mN/m, respectively), the conformation of the surfactant molecules seem to be different. The average parking areas of the P123 molecules on the air-DW and air-SBF interfaces estimated from the figure using the Gibbs adsorption equation are 0.60 and 0.51 nm^2, respectively. It seems that the higher ionic strength of the SBF causes a more compact monomer structure most probably through the depression of the localized electric charges on the surfactant molecules by the stronger ionic environment. The charge suppression also seems to promote early aggregation and lowers the transition concentration between monomers and molecular aggregates. These findings are in agreement with the reported micellar behavior observed in other polyelectrolyte solutions [42].

The surface tension result summarized in Fig. 1 were the basis for selecting the optimum P123 concentration of 10^{-3} M to generate the micelles for the subsequent dilution tests. The concentration selected is high enough to ensure the formation of tight, spherical micelles whereas it is low enough that the transition to the cylindrical micelle form, which is known to take place after 10^{-2} M [43] is not allowed.

The surface tension tests in the DW and SBF solutions were repeated in the presence of 10^{-4} M BSA with no observable differences compared to the surface tension profiles presented in Fig. 1. It is known that the BSA adsorbs at the air-water interface rather weakly with an equilibrium surface tension of about 50 mN/m [44,45]. This suggests that the surfactant molecules which are much more readily adsorbed at the interface blanket any effects due to the larger, less surface active protein molecules.

3.1.2. Size and surface charge measurements

The literature data states that the radii of the micelles of the Pluronic series polymeric surfactants varies between 10–20 nm depending on the relative length of the PEO and PPO chains and on the measurement method. Raval et al. [34] and Cihan et al. [57] reported that the apparent average radii of the P123 micelles were around 10 nm [34,57]. According to Brown et al. [36], the hydrodynamic radii of the micelles of the P85 with smaller hydrophobic sections were 9.3 nm at ambient temperature. Zhou and Chu [37] observed similar values for P188 with still smaller hydrophobic segments (PEO_{80}-PPO_{25}-PEO_{80}) as 8.0 nm.

Fig. 2-a presents the size distributions of the P123 micelles in 10^{-3} M DW and SBF solutions obtained by the DLS measurements. Interestingly, there is not a significant change in the size distributions for both cases. The mean spherical diameters of the micelles were found to be 18.3 nm for both cases and are quite similar to those observed by Ashraf et al. [46]. These authors observed by DLS that the hydrodynamic diameter of P123 was 14.3 nm at 25 °C in water at a P123 concentration of 4.2×10^{-2} M. These diameters are lower than that observed by Raval et al. 34. who recently reported a DLS mean size of 21.7 nm for the micelles at a P123 concentration of 1.7×10^{-3} M at 25 °C. Though the mean sizes reported by these two groups place our measurements in the middle, it should be kept in mind that the actual sizes of the micelles must show a distribution around these means as demonstrated by Fig. 2-a.

Our direct visual observations of the 10^{-3} M P123 micelles in DW and SBF using STEM and AFM are presented in Fig. 3. The figure clearly illustrates the spherical shapes of the micelles. A closer inspection of the STEM figure on the right gives a size range between 20–50 nm, supporting the DLS distribution presented in Fig. 2-a.

Zeta potential measurements of the P123 micelles measured in DW and SBF at 10^{-3} M are presented in Fig. 2-b. The figure shows that the charge distribution of the micelle population is wider in the case of DW (ranging from -35 to +45 mV) with the mean zeta potential is at around 0 mV, indicating the average non-ionic nature of the copolymer. The charge distribution becomes narrower in the SBF solution (between -25 and +20 mV) with the mean zeta potential is at -10 mV. The significant shift to the negative side is most probably due to the suppression of highly charged sites on the micelles by the ionic species present in the SBF electrolyte. Similar behavior was observed by Farace et al. [47] with Pluronic F68 where the addition of a double-valenced $CaCl_2$ caused coagulation of the micelles due to the suppression of the original negative charge on the molecules [47]. The addition of NaCl was not able to bring any stabilization, however. It seems that the suppression of the charges in SBF solution from -35/+45 mV range to -25/+20 mV range is not sufficient to lead to significant aggregation among the micelles as observed by the size distribution data presented in Fig. 2-a.

3.2. Characterization of BSA in DW and SBF solutions

With 42 g/L, serum albumins are the most abundant proteins in the blood plasma, accounting for about 60 % of the total protein concentration. Albumins display an affinity for binding to a variety of lipophilic ligands such as fatty acids, lysolecithin, bilirubin, warfarin, tryptophan, steroids, anesthetics and several dyes [48]. Hence, they play an important role in the transport and deposition of a variety of endogenous and exogenous substances in the blood [49,50]. The albumins are also known to strongly interact with surfactants so much so that some ionic surfactants have been employed through different spectroscopic techniques to elucidate details of the protein structure and binding mechanism [48,51]. Therefore, their interactions with drug-carrying micelles and the possible effects on the micellar stability should be taken very seriously.

In this work, the BSA was employed to investigate its effect on the stability of the P123 micelles. The bovine serum albumin (BSA), which is a globular protein with the approximate shape of a prolate spheroid of dimensions $4 \times 4 \times 14$ nm, corresponding to an equivalent volume diameter of 6.1 nm 44., displays biological homology to the human serum albumin (HSA). It is widely employed as an HSA replacement in many biochemical and pharmacological applications because of its low cost and ready availability [52,53].

The DLS size distributions of the 10^{-4} M BSA in DW and SBF solutions are presented in Fig. 4-a. The mean size of the BSA molecules was measured to be 5.2 nm in DW and 7.3 nm in SBF, which is in close agreement with the literature reported values [43,44,54]. Changing the protein concentration to 10^{-2} M and 10^{-5} M did not have a significant influence on the size distribution and not reported here in graphical form.

With an isoelectric point (IEP) around pH 4.5–5.0, BSA is dominantly negatively charged in neutral pH [55,56]. The zeta potential distribution of BSA in DW obtained with DLS-LDV at the physiological pH of 7.4 is presented in Fig. 4-b. The figure shows that the BSA molecules are charged negatively at this pH in distilled water as expected and have a mean negative zeta potential of about −25 mV. Charging of

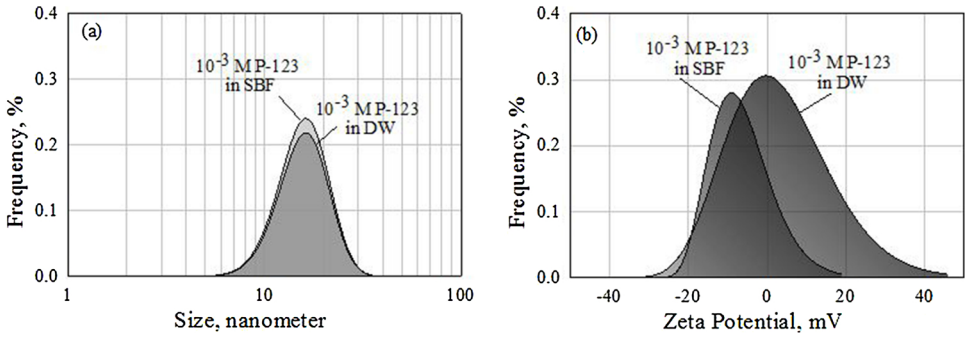

Fig. 2. The size (a) and zeta potential (b) distributions of the 10^{-3} M P123 micelles in DW and SBF solutions. (The mean size in the figures coresspond to 16.3 nm in both cases).

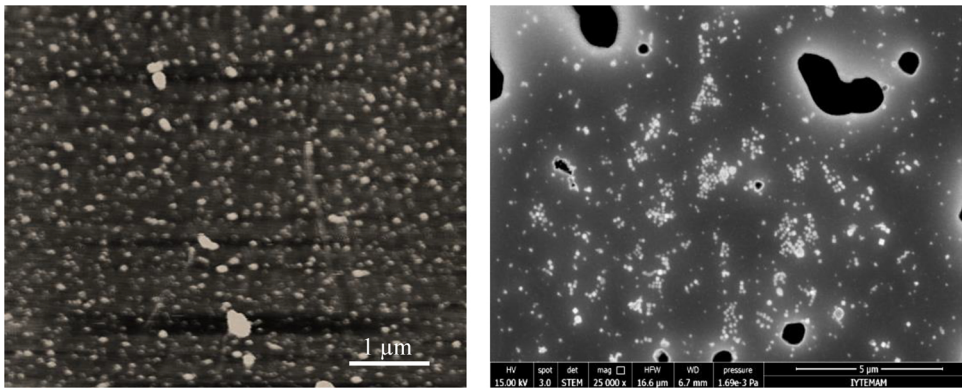

Fig. 3. The appearance of the 10^{-3} M P123 micelles in DW using AFM (left) and in SBF using STEM (Right).

BSA in the SBF solution is also presented in Fig. 4-b and presents quite different behavior with the mean zeta potential shifting towards zero. The observed suppression of the local negative charges on the BSA molecules in SBF most probably is the reason for the mild aggregation observed in the size distributions presented in Fig. 4-a.

The size and morphology of the BSA molecules in SBF were examined using AFM and STEM scanning for further analysis. The representative pictures are presented in Fig. 5. Aggregated BSA molecules are clearly visible in the inset of the STEM picture, confirming directly the results of the size and charge measurements presented in Fig. 4.

3.3. Micelle stability upon dilution in DW and SBF

DLS measurements were carried out to determine the influence of systematic re-dilution of the DW and SBF micellar solutions to lower concentrations on the micelle stability. The concentration range of the 10^{-3} M P123 stock solutions after dilution was between 10^{-3} M (no dilution, i.e. the stock solution itself) and 10^{-7} M (the highest dilution). The tests were carried out in the absence and presence of inter-micellar (i.e. the BSA in the dilution solution) and intra-micellar (i.e. probucol within the micelle structure) species separately or together. The results are presented in Figs. 6 and 7, collectively.

3.3.1. In the absence of BSA (no probucol)

The results of diluting the 10^{-3} M P123 DW and SBF micellar solutions to lower concentrations in the absence of any inter-micellar (BSA) and intra-micellar (probucol) species are presented in Fig. 6-a and -b, respectively.

In the case of DW, the size distribution observed at 10^{-3} M P123 solution gradually shifts to finer sizes (Fig. 6-a). The shift which is slow and relatively small initially upon dilution to 10^{-4} M and 10^{-5} M quickly becomes very fine when the solution diluted to 10^{-6} M and 10^{-7} M. The behavior is quite different when the same dilution procedure is applied to the SBF micellar solution (Fig. 6-b). Though the micelle size in SBF is similar to that of DW at 10^{-3} M (see also Fig. 2), dilution to 10^{-4} and 10^{-5} M causes a growth in the apparent size of the

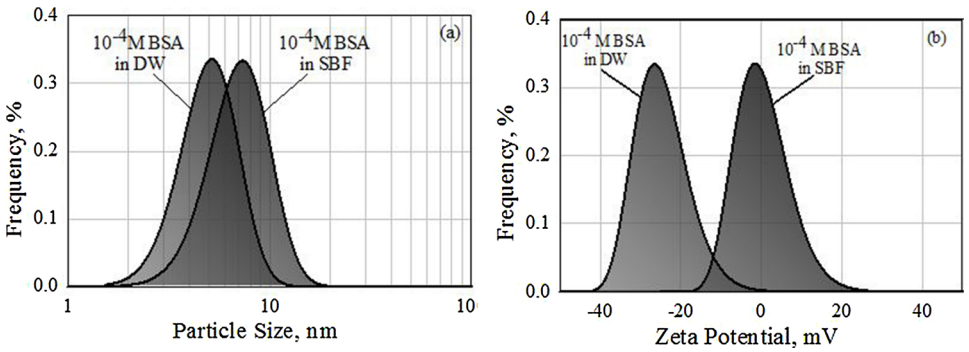

Fig. 4. The size (a) and the zeta potential (b) distributions of the 10^{-4} M BSA in DW and SBF solutions.

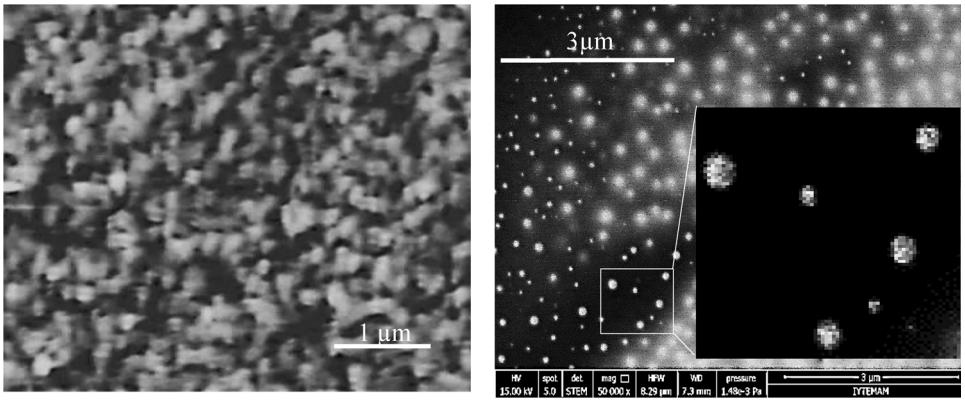

Fig. 5. The appearance of the 10^{-4} M BSA molecules observed using AFM and STEM.

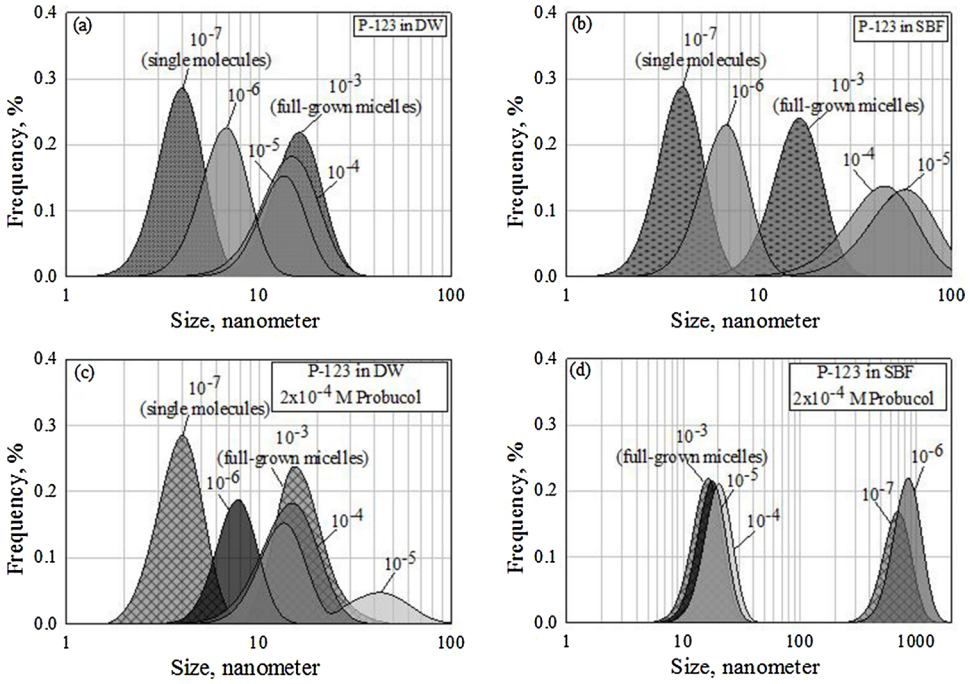

Fig. 6. The size distributions of the barren and drug-loaded P123 micelles in DW and SBF solutions after dilution in the absence of BSA.

micelles in the SBF solutions. The growth in size in these dilutions may be indicative of extensive swelling as reported by Alexandridis and Hatton [38] that dynamic light scattering detects the micelle hydrodynamic radius which includes the water hydrating the EO segments. The lowered local charges observed in the case of SBF (see Fig. 2) may be the cause of a loose aggregation which leads to the swollen micelles with mean sizes reaching upto 60 nm. Further ten-fold dilution to 10^{-6} M causes a precipitous drop in the micelle size, a clear indication of the disintegration of these swollen structures. Another ten-fold decrease in concentration brings the mean size (diameter) down to 4 nm. This observed radius of 2 nm is nearly the same as the molecular radii reported by Raval et al. [34], Brown et al. [36], Zhou and Chu [37] and Mortensen et al. [39]. The dilution test results show clearly that the compact micelles observed above the CMC will break up to primary constitutive molecules when dilution reaches below the onset concentration for forming the molecular aggregates (dimers, trimers, etc). The results further demonstrate that the compact micelles swell significantly before unfolding and eventually disintegrating into individual molecules in the case of the simulated body fluids.

3.3.2. *In the presence of 10^{-4} M BSA (no probucol)*

The dilution of the 10^{-3} M P123 DW and SBF micellar solutions tests were repeated in the presence of 10^{-4} M BSA to observe the sole effect of inter-micellar protein molecules on micellar stability. This concentration of the protein was selected since it is close to the body concentration which ranges between 4.5×10^{-4} and 7.5×10^{-5} M [12]. The results are presented in Fig. 7-a and -b for DW and SBF solutions, respectively. Though the size distributions of the full-grown micelles at 10^{-3} M stock solution of P123 are very similar to those observed for the no BSA case (see Fig. 6-a and -b) for both the DW and SBF solutions, the results show significantly different behavior in the presence of BSA compared to the dilution tests carried out in the absence of BSA. In the case of DW solutions, the micelles disintegrate to primary molecules more quickly starting at 10^{-5} M and further dilution does not cause any more effect. It seems that both the surfactant molecules and BSA retain their individuality. In the case of SBF, however, dilution starts its effect at 10^{-4} M and the mean size decreases to around 7 nm and remains nearly constant with further dilution. This size is similar to the mean size of the BSA aggregates observed in SBF solutions (see also Fig. 4). The absence of a peak at around 4 nm (size of a single P123 molecule) suggests that the unfolded P123 molecules are in contact with the larger protein molecules most probably due to the charging state of both molecules favoring closer approach (see Figs. 2 and 4).

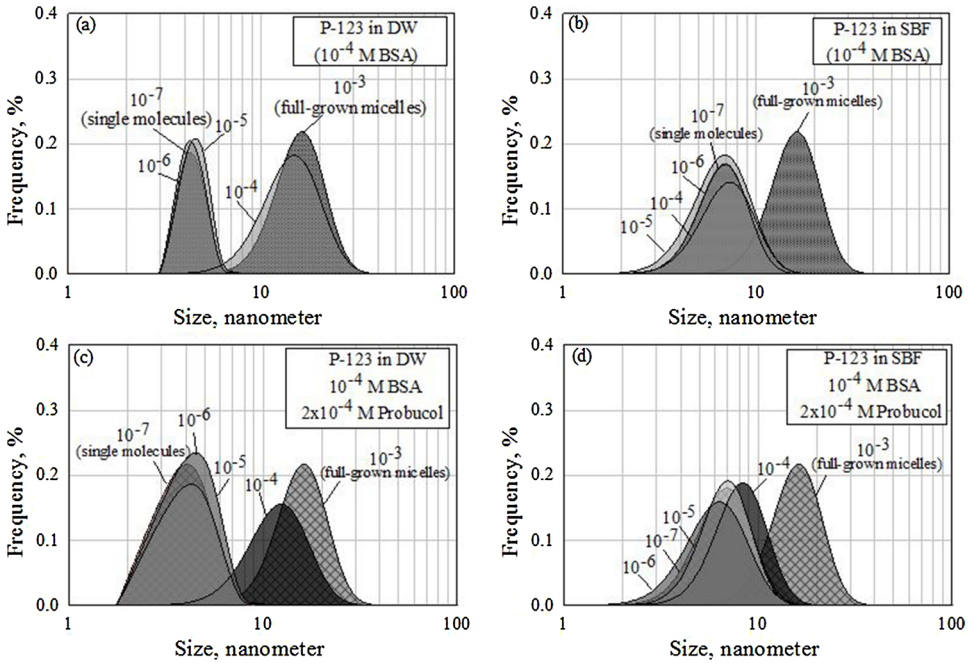

Fig. 7. The size distributions of the barren and drug-loaded P123 micelles in DW and SBF solutions after dilution in the presence of 10^{-4} M BSA.

Lowering the BSA molar concentration to 10^{-5} resulted in similar behavior with the difference that the micelle integrity was disrupted at a higher dilution ratio. Increasing the molar concentration of the BSA to 10^{-3} M where it had 1:1 M ratio with the P123 molecules led to an opposite behavior. It seems that at 10^{-3} M BSA (which is above the higher end of the body concentration) the integrity of the formed micelles was disrupted to the degree that micelles seem to disintegrate even without any dilution. For the sake of clarity, the figures for different BSA concentrations are not presented here.

3.3.3. *In the absence of BSA (with 10^{-4} M probucol)*

The tests in the above paragraphs were repeated with probucol loaded micelles in DW and SBF solutions in the absence of the protein to determine the effect of *intra-micellar* species on micelle stability. A representative TEM image of the P123 micelles in DW loaded with probucol is given in Fig. 8. The photograph clearly shows that the drug was successfully incorporated into the micellar cores.

A comparison of Fig. 6-a and -c shows that the presence of the drug in the full-grown micelle structure at 10^{-3} M P123 concentration does not influence the size of the micelles. The behavior for the DW solutions in the absence of protein is similar to whether the micelles were loaded with the drug or not except for the dilution concentration of 10^{-5} M P123 where large aggregates seem to be forming. The aggregation trend continues with the P123 solution of 10^{-6} M, but to a lesser extent. The final dilution concentration of 10^{-7} M creates single P123 molecules irrespective of whether probucol was present in the system.

The dilution response of the micelles was, however, grossly different if the probucol loaded micelles were in SBF solutions (Fig. 6-b and -d). Though the size distributions of the full-grown micelles were very similar at 10^{-3} M P123 concentration, at dilution levels below 10^{-5} M nearly micron-sized structures develop in SBF solution when probucol is present. It may be possible that the lipophilic drug acts as a binder for the P123 molecules as they unfold from the micellar structure at high dilution (where it is known that micelles start to disintegrate), creating loosely connected P123 polymeric structures. The observed loose aggregation behavior does not hide the fact that micelle disintegration upon dilution is not affected by the presence of a lipophilic drug in the micelle structure.

3.3.4. *In the presence of 10^{-4} M BSA (with 10^{-4} M probucol)*

The size of the full-grown micelles in 10^{-3} M P123 solution was not affected when probucol was loaded into the micelles whether in DW and SBF solutions in the presence of 10^{-4} M BSA (Fig. 7-c and d). In the SBF-BSA solutions (Fig. 7-b and -d), the effect of dilution is similar whether the micelles were loaded with the drug. The dilution starts its effect at 10^{-4} M and the mean size gradually decreases to around 7 nm as in the case of barren micelles at 10^{-7} M P123, which is the mean size of the BSA aggregates observed in SBF solutions (see Fig. 4). The absence of a peak at around 4 nm (size of a single P123 molecule) suggests that the unfolded P123 molecules are in contact with the larger protein molecules.

The behavior of the loaded micelles upon dilution in the presence of DW-BSA solutions is surprising (Fig. 7-a and -c). Again, the size decreases with dilution but the effect is drastic at dilution levels below 10^{-4} M P123. The interesting observation is that the mean of the size distribution of the P123/BSA/probucol system is around 4.0 nm at P123 dilution concentrations between 10^{-5} M and 10^{-7} M, which is about the size of the single P123 molecule and the effect of the BSA molecules do not show in the overall distribution.

Nevertheless, similar to the case with the no BSA, the above results demonstrate unequivocally that dilution leads to the disintegration of the micelles in the presence of BSA and whether a lipophilic drug was present in the micellar cores. The findings of the study demonstrate that dilution effects must be taken into account in devising drug carriers from polymeric surfactant aggregates and that the presence of lipophilic drug acting as a binder in the hydrophobic core may not always be sufficient to hold the micelles intact during dilution as suggested by previous studies [1,13,58–60]. The one solution to the problem would be the encapsulation of the micelles within a sturdier shell as demonstrated by the authors of this paper in previous work [57,61] where spherical chitosan nano-shells were employed to envelop micelles for solvation and safeguarded delivery of a strongly lipophilic drug.

4. Conclusions

In this study, the effect of systematic re-dilution of the P123 micelles from 10^{-3} M micellar stock solutions to lower concentrations (ranging between 10^{-3} M and 10^{-7} M) on the micellar stability was

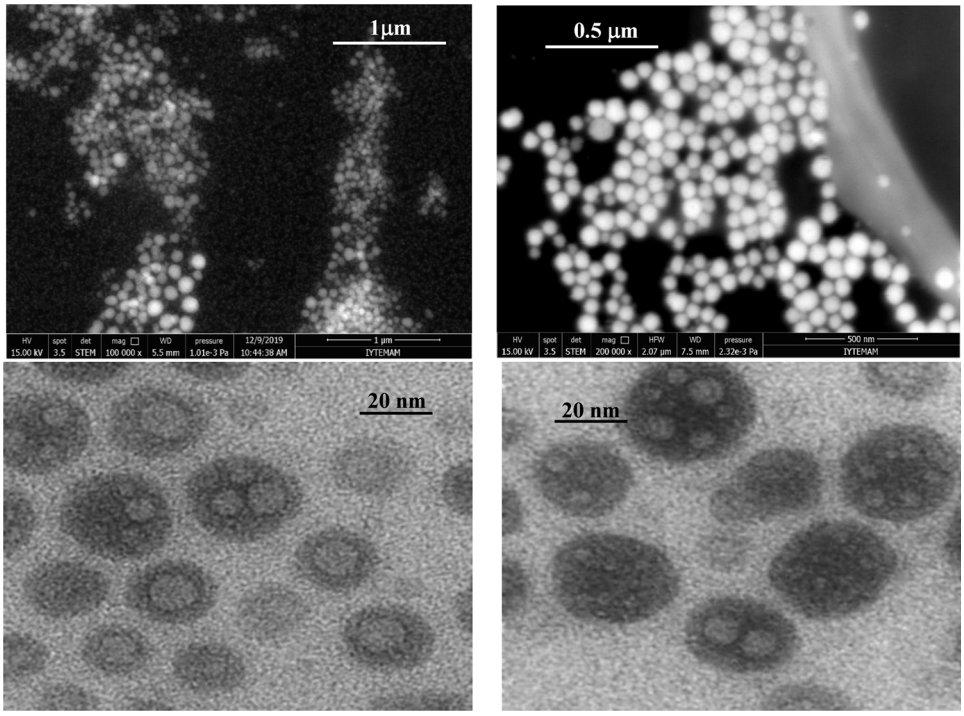

Fig. 8. STEM images of the drug-loaded P123 micelles at different magnifications (top figures) and the TEM images of the drug-loaded P123 micelles in DW (bottom figures).

investigated. The tests were carried out in the absence and presence of inter- and intra-micellar species, the protein BSA, and the lipophilic drug probucol, respectively. Characterization of the micelles was carried out using DLS, AFM, STEM, and TEM.

The findings of the study demonstrated unequivocally that

- The formed micelles from the 10^{-3} M P123 stock solution show varying degrees of disintegration upon dilution.
- the presence of inter (the protein BSA in solution) or intra (the drug probucol within the core) micellar species could not prevent the disintegration of the micelles upon dilution. The same was true when the BSA and the probucol were simultaneously present.
- Increasing concentration of the protein BSA seems to cause disruption at lower dilution levels such that above a certain value the micelles disintegrate even without dilution.

Funding

Financial support for this work was provided by the Izmir Institute of Technology Scientific Research Projects Fund (IYTE-BAP).

Declaration of Competing Interest

No conflict of interest exists.

Acknowledgments

We thank the Material Research Center of the Integrated Research Centers of Izmir Institute of Technology for performing the STEM and AFM analyses.

References

[1] G. Gaucher, M.H. Dufresne, V.P. Sant, N. Kang, D. Maysinger, J.C. Leroux, Block copolymer micelles: preparation, characterization and application in drug delivery, J. Control. Release 109 (2005) 169–188.
[2] K. Sachs-Barrable, S.D. Lee, E.K. Wasan, S.J. Thomton, K.M. Wasan, Enhancing drug absorption using lipids: a case study presenting the development and pharmacological evaluation of a novel lipid-based oral amphotericin B formulation for the treatment of systemic fungal infections, Adv. Drug Deliv. Rev. 60 (2007) 692–701.
[3] L. Plapied, N. Duhem, A. des Rieux, V. Preat, Fate of polymeric nanocarriers for oral drug delivery, Curr. Opin. Colloid Interface Sci. 16 (2011) 228–237.
[4] A.C. Hunter, J. Elsom, P.P. Wibroe, S.M. Moghimi, Polymeric particulate technologies for oral drug delivery and targeting: a pathophysiological perspective, Nanomed. Nanotechnol. Biol. Med. (2012) 5–20.
[5] L.M. Ensign, R. Cone, J. Hanes, Oral drug delivery with polymeric nanoparticles: the gastrointestinal mucus barriers, Adv. Drug Deliv. Rev. 64 (2012) 557–570, https://doi.org/10.1016/j.addr.2011.12.009.
[6] H. Maeda, H. Nakamura, J. Fang, The EPR effect for macromolecular drug delivery to solid tumors: improvement of tumor uptake, lowering of systemic toxicity, and distinct tumor imaging in vivo, Adv. Drug Deliv. Rev. 65 (2013) 71–79.
[7] Z. Xu, K. Graham, M. Foote, F. Liang, R. Rizkallah, M. Hurt, Y. Wang, Y. Wu, Y. Zhou, 14-3-3 protein targets misfolded chaperone-associated proteins to aggresomes, J. Cell. Sci. 126 (2013) 4173–4186.
[8] P. Talelli, W. Waddingham, A. Ewas, J.C. Rothwell, N.S. Ward, The effect of age on task-related modulation of interhemispheric balance, Exp. Brain Res. 186 (2008) 59–66.
[9] I. Lynch, T. Cedervall, M. Lundqvist, C. Cabaleiro-Lago, S. Linse, K.A. Dawson, The nanoparticle–protein complex as a biological entity; a complex fluids and surface science challenge for the 21 st century, Adv. Colloid Interface Sci. 135 (2007) 167–174.
[10] A.E. Nel, L. Madler, D. Velegol, T. Xia, E.M. Hoek, P. Somasundaran, F. Klaessig, V. Castranova, M. Thompson, Understanding biophysicochemical interactions at the nano-bio interface, Nat. Mater. 8 (2009) 543–557.
[11] K. Nešporová, J. Šógorkováa, D. Šmejkalováa, J. Kulháneka, G. Huerta-Angelesa, L. Kubalab, V. Velebnýa, Influence of serum albumin on intracellular delivery of drug-loaded hyaluronan polymeric micelles, Int. J. Pharm. 511 (2016) 638–647.
[12] Harmonisation of Reference Intervals (https://web.archive.org/web/20130802082027/ http:/www.acb.org.uk/docs/Pathology Harmony for web.pdf) Pathology Harmony. Archived from the original (PDF) on 2 August 2013. Retrieved 23 June 2013.
[13] A.V. Kabanov, E.V. Batrakova, V.Y. Alakhov, Pluronic block copolymers as novel polymer therapeutics for drug and gene delivery, J. Control. Release 82 (2002) 189–212.
[14] J. Yaneva, S.H. Leuba, K. Van Holde, J. Zlatanova, The major chromatin protein histone H1 binds preferentially to cis-platinum- damaged DNA (anticancer drugsyDNA adductsyHMG1ylinker histones), Proc. Natl. Acad. Sci. 94 (1997) 13448–13451.
[15] Y. Jiang, C. Zhu, L. Ling, L. Wan, X. Fang, C. Bai, Specific aptamer-protein interaction studied by atomic force microscopy, Anal. Chem. 75 (2003) 2112–2116.
[16] G. Wang, Z. Nikolovska-Coleska, C.Y. Yang, R. Wang, G. Tang, J. Guo, S. Shangary, S. Qiu, W. Gao, D. Yang, J. Meagher, J. Stuckey, K. Krajewski, S. Jiang, P.P. Roller, H. Ozel Abaan, Y. Tomita, S. Wang, Structure- based design of potent Sm all-molecule inhibitors of anti-apoptotic Bcl-2 proteins, J. Med. Chem. 49 (2006) 6139–6142.

[17] J. Xu, Y. Li, Discovering disease-genes by topological features in human protein–protein interaction network, Oxf. J. 22 (2006) 2800–2805.

[18] Y.D. Ivanov, P.A. Frantsuzov, A. Zöllner, N.V. Medvedeva, A. Archakov, W. Reinle, R. Bernhardt, Atomic force microscopy study of protein–protein interactions in the cytochrome CYP11A1 (P450scc)-Containing steroid hydroxylase system, Nanoscale Res. Lett. 6 (2011) 54.

[19] T. Ando, T. Uchihashi, N. Kodera, A. Miyagi, R. Nakakita, H. Yamashita, M. Sakashita, High-speed atomic force microscopy for studying the dynamic behavior of protein molecules at work, J. Appl. Phys. 45 (2006) 1–3.

[20] E.Y. Mayyas, Investigation of Protein-Protein Interaction Using Atomic Force Microscopy, PhD Dissertation Nanomechanics Laboratory, Department of Physics and Astronomy, Wayne State University, Detroit, 2011.

[21] F.S. Kao, W. Ger, Y.R. Pan, H.C. Yu, R.Q. Hsu, H.M. Chen, Chip-based protein–Protein interaction studied by atomic force microscopy, Biotechnol. Bioeng. 109 (2012) 2460–2467.

[22] M. Tribout, S. Paredes, M.J. González-Mañas, F.M. Goñi, Binding of Triton X-100 to bovine serum albumin as studied by surface tension measurements, J. Biochem. Biophys. Methods 22 (1991) 129–133.

[23] W. Kevin, P. Mattison, L. Dubin, I.J. Brittain, Complex formation between bovine serum albumi,n and strong polyelectrolytes: effect of polymer charge density, J. Phys. Chem. B 102 (1998) 3830–3836.

[24] A. Valstar, M. Almgren, W. Brown, M. Vasilescu, The interaction of bovine serum albumin with surfactants studied by light scattering, Langmuir 16 (2000) 922–927.

[25] S.F. Santos, D. Zanette, H. Fischer, R. Itri, A systematic study of bovine serum albumin (BSA) and sodium dodecyl sulfate (SDS) interactions by surface tension and small angle X-ray scattering, J. Colloid Interface Sci. 262 (2003) 400–408.

[26] S. Bianca, Z. Dino, I. Rosangela, Bovine serum albumin (BSA) plays a role in the size of SDS micelle-like aggregates at the saturation binding: the strength effect, J. Colloid Interface Sci. 277 (2004) 285–291.

[27] C.L. Mesa, Polymer–surfactant and protein–surfactant interactions, J. Colloid Interface Sci. 286 (2005) 148–157.

[28] É. Kiss, K. Dravetzky, K. Hill, E. Kutnyánszky, A. Varga, Protein interaction with a Pluronic-modified poly(lactic acid) Langmuir monolayer, J. Colloid Interface Sci. 325 (2008) 337–345.

[29] P. Opanasopit, M. Yokoyama, M. Watanabe, K. Kawano, Y. Maitani, T. Okano, Influence of serum and albumins from different species on stability of camptothecin-loaded micelles, J. Control. Release 104 (2005) 313–321.

[30] S.C. Owen, C.P.Y. Dianna, M.S. Shoichet, Polymeric micelle stability, Nano Today 7 (2012) 53–65.

[31] Y. Shi, T. Lammers, G. Storm, W.E. Hennink, Physico-chemical stability and drug retention of polymeric micelles for tumor-targeted drug delivery, Macromol. Biosci. 7 (2017) Feature Article.

[32] W. Zhou, C. Li, Z. Wang, W. Zhang, J. Liu, Factors affecting the stability of drug-loaded polymeric micelles and strategies for improvement, J. Nanopart. Res. 18 (2016) 275–293.

[33] M.Y. Kozlov, N.S. Melik-Nubarov, E.V. Batrakova, A.V. Kabanov, Relationship between pluronic block copolymer, structure, critical micellization concentration and partitioning coefficients of low molecular mass solutes, Macromolecules 33 (2000) 3305–3313.

[34] A. Raval, S.A. Pillai, A. Bahadur, P. Bahadur, Systematic characterization of Pluronic micelles and their application for solubilization and in vitro release of some hydrophobic anticancer drugs, J. Mol. Liq. 230 (2017) 473–481.

[35] A. Oyane, H.M. Kim, T. Furuya, T. Kokubo, T. Miyazaki, T. Nakamura, Preparation and assesment of revised simulated body fluids, J. Biomed. Mater. Res. 65 (2003) 188–195.

[36] W. Brown, K. Schilllen, M. Almgren, S. Hvidt, P. Bahadur, Micelle and gel formation in a poly(ethylene oxide)/poly (propylene oxide)/poly(ethy1ene oxide) triblock copolymer in water solution. Dynamic and static light scattering and oscillatory shear measurements, Am. J. Phys. Chem. 95 (1991) 1850–1858.

[37] Z. Zhou, B. Chu, Light-scattering study on the association behavior of triblock polymers of ethylene oxide and propylene oxide in aqueous solution, J. Colloid Interface Sci. 126 (1988) 171–180.

[38] P. Alexandridis, T. Alan Hatton, Poly(ethylene oxide)-poly(propylene oxide)-poly (ethylene oxide) block copolymer surfactants in aqueous solutions and at interfaces: thermodynamics, structure, dynamics, and modeling, Colloids Surf. A Physicochem. Eng. Asp. 96 (1995) 1–46.

[39] K. Mortensen, W. Brown, B. Norden, Inverse melting transition and evidence of 3-dimensional cubatic structure in a block-copolymer micellar system, Phys. Rev. Lett. 68 (1992) 2340–2343.

[40] H. Polat, S. Chander, Adsorption of PEO/PPO triblock copolymers and wetting of coal, Colloids Surf. A Physicochem. Eng. Asp. 146 (1999) 199–212.

[41] A. Asnacious, D. Langevin, J.-F. Argillier, Complexation of cationic surfactant and anionic polymer at the air-water interface, Macromolecules 29 (1996) 7412–7417.

[42] P. Petrov, J. Yuan, K. Yoncheva, A.H.E. Müller, C.B. Tsvetanov, Wormlike morphology formation and stabilization of “Pluronic P123” micelles by solubilization of pentaerythritol tetraacrylate, J. Phys. Chem. B 112 (2008) 8879–8883.

[43] B. Lorber, F. Fischer, M. Bailly, H. Roy, D. Kern, Protein analysis by dynamic light scattering: methods and techniques for students, Biochem. Mol. Biol. Educ. 40 (2012) 372–382.

[44] S.J. McClellan, E.I. Franses, Effect of concentration and denaturation on adsorption and surface tension of bovine serum albumin, Colloids Surf. B Biointerfaces 28 (2003) 63–75.

[45] D. Guzey, I. Gulseren, B. Bruce, J. Weiss, Interfacial properties and structural conformation of thermosonicated bovine serum albumin, Food Hydrocoll. 20 (2006) 669–677.

[46] U. Ashraf, O.A.M. Chat Maswal, S. Jabeen, A. Dar Ahmad, An investigation of Pluronic P123–sodium cholate mixed system: micellization, gelation and encapsulation behavior, RSC Adv. 5 (2015) 83608–83618.

[47] C. Farace, P. Sánchez-Moreno, M. Orecchioni, R. Manetti, F. Sgarrella, Y. Asara, M. José, P. García, J.A. Marchal, R. Madeddu, L.G. Delogu, Immune cell impact of three differently coated lipid nanocapsules: pluronic, chitosan and polyethylene glycol, Nature Sci. Rep. 6 (2016) 18423, https://doi.org/10.1038/srep18423.

[48] H.D. Carter, J.X. Ho, Advances in Protein Chemistry Vol. 45 Academic Press, New York, 1994, pp. 153–203.

[49] I.T. Kosa, T. Maruyama, M. Otagiri, Species differences of serum albumins: I. Drug binding sites, Pharm. Res. 14 (1997) 1607–1612.

[50] J.F. Moreno, M. Cortijo, J.G. Jimenez, Interaction of acrylodan with human serum albumin. A fluorescence spectroscopic study, Photochem. Photobiol. 69 (1999) 8–15.

[51] E.L. Gelamo, C.H.T.P. Silva, H. Imasato, M. Tabak, Interaction of bovine (BSA) and human (HSA) serum albumins with ionic surfactants: spectroscopy and modelling, Biochim. Biophys. Acta 1594 (2002) 84–99.

[52] J.L. Sohl, A.G. Aplittgerber, The binding of coomassie brilliant blue to bovine serum albumin: a physical biochemistry experiment, J. Chem. Edu. 68 (1991) 262–264.

[53] C. Liua, W. Yanga, Q. Gaoa, J. Dua, H. Luoa, Yi. Liub, C. Yang, Differential recognition and quantification of HSA and BSA based on two red-NIR fluorescent probes a, J. Lumin. Appl. 197 (2018) 193–199.

[54] Y. Li, G. Yang, Z. Mein, Spectroscopic and dynamic light scattering studies of the interaction between pterodontic acid and bovine serum albumin, Acta Pharm. Sin. B 2 (2012) 53–59.

[55] S. Servagent-Noinville, M. Revault, H. Quiquampoix, M.H. Baron, Conformational changes of bovine serum albumin induced by adsorption on different clay surfaces: FTIR analysis, J. Colloid Interface Sci. 221 (2000) 273–283, https://doi.org/10.1006/jcis.1999.6576 WOS:000084997300019. PMID: 10631031.

[56] T. Kopac, B.K. ozgeyik, J. Yener, Effect of pH and temperature on the adsorption of bovine serum albumin onto titanium dioxide, Colloid Surf. A 322 (2008) 19–28 WOS:000257129300004.

[57] E. Cihan, M. Polat, H. Polat, Designing of spherical chitosan nano-shells with micellar cores for solvation and safeguarded delivery of strongly lipophilic drugs, Colloid Surf. A 529 (2017) 815–823.

[58] E.V. Batrakova, A.V. Kabanov, Pluronic block copolymers evolution of drug delivery concept from inert nanocarriers to biological response modifiers, J. Control. Release 130 (2008) 98–106, https://doi.org/10.1016/j.jconrel.2008.04.013.

[59] Y. Lu, E. Zhang, J. Yang, Z. Cao, Strategies to improve micelle stability for drug delivery, Nano Res. 11 (2018) 4985–4998, https://doi.org/10.1007/s12274-018-2152-3.

[60] R. Trivedi, U.B. Kompell, Nanomicellar formulations for sustained drug delivery: strategies and underlying principle, Nanomedicine (Lond.) 5 (2010) 485–505, https://doi.org/10.2217/nnm.10.10.

[61] M. Polat, H. Polat, Recent advances in chitosan-based systems for delivery of anticancer drugs, in: S. Jana, S. Jana (Eds.), Functional Chitosan: Drug Delivery and Biomedical Applications, Spring Nature, 2020, pp. 191–228.